48th AIAA/ASME/ASCE/AHS/ASC Structures, Structural Dynamics, and Materials Conference
23 - 26 April 2007, Honolulu, Hawaii

AIAA 2007-2176

An Approach to Preliminary Design and Analysis

Craig Collier[1], Phil Yarrington[2], Mark Pickenheim[3], and Brett Bednarcyk[4]
craig.collier@hypersizer.com
Collier Research Corp., Hampton, VA 23669

A process of performing high fidelity aerospace structural analyses early in the design cycle is presented. The process has been programmed into a tool called HyperFEA™ and couples the software HyperSizer® for failure analysis methods and sizing optimization with FEA to provide a robust system that is capable of exploring very rapidly a large design space of different FEM geometries, panel concepts, material selections, cross sectional dimensions, and composite layups for airframes and launch vehicles. The software includes hundreds of different analyses such as panel buckling, crippling, bonded and bolted joint, and composite strength to both lamina and laminate methods using damage tolerance criteria and corresponding test data correlation for consistently establishing margins-of-safety for airworthiness certification. Several examples are provided ranging from cylindrical launch structure, that does not need FEA, to a wing box that is optimized in an iterative manner with HyperSizer and FEA to a prescribed wing tip deflection. Design shortcomings are avoided and more robust designs are found as the software is used throughout four different levels of progressive analysis and design.

[1,2,3,4] Senior Research Engineers, Hampton, Virginia, AIAA Senior Members.

1 Introduction

Two fundamental classes of structures are considered. The first is structure such as the tanks, interstages, skirts, and frustums of the NASA Crew Launch Vehicle (CLV), Fig 1, which can be analyzed with internal loads calculated with closed form equations. In these cases a FEM is not required to derive appropriate design-to loads and Excel spreadsheets can be used in an efficient way to allow configuration geometry such as diameter to change dynamically with the calculated compressive running forces caused by bending moments of the stack. Simple equations were defined to calculate the design-to internal loads on the cylindrical Outer Mold Line (OML) panels of launch vehicle structure. For this type of structure, a design-space exploration was performed very rapidly without needing to build a FEM.

There were two loadings considered: ascent thrust load causing pure uniaxial compression on the cylindrical shell, and a wind gust causing shear and a bending moment in the stack resulting in peak compression forces and in-plane shear. If the cylindrical structure also contained ringframes, then the Poisson's coupling effect of the ringframes generate a small component of compression force transverse to the panels. This compressive transverse (–Ny) loading component was included with the primary axial compression (-Nx) load. Instead, of using FEA, these two loadings were calculated in an Excel spreadsheet as a function of geometry input, then automatically fed into the Free Body Diagram (FBD) tab through HyperSizer's Object Model.

Geometry (INPUT)		**Geometry (OUTPUT)**	
Thickness	0.60	Panel Spacing Height	28.23
Diameter	144.80	Panel Spacing Width	75.82
Radius of Curvature	72.40		
Height	84.70	**Cross section (OUTPUT)**	
# Ringframes	3.00	Moment of Inertia	706482.86
# Longerons	6.00	Unit Force from moment (peek)	-8054.89
		Unit Force from axial	-3561
		Moment multiplier	6.149E-05
Loads (INPUT)			
		Load (OUTPUT)	
Axial	-1620000.00	External Moment	-1.310E+08
Shear	60000.00	AXIAL Internal Load	
Moment (a)	-131000000.00	Strength	-11616
		Buckling	-10537
		SHEAR Internal Load	
		Strength	528
		Buckling	352

Figure 2, Corresponding spreadsheet of loads.

The second class of structure, which are more common in aerospace, do require FEA to predict internal load paths and to establish appropriate design-to forces. The NASA Crew Exploration Vehicle (CEV) falls in this class as do the fuselages and wings of airframes. For this paper, a wing box of a representative commercial transport is presented to illustrate the process of coupling closed form analysis with FEA and the resulting impacts to margins and weights for not including appropriate failure modes in the early preliminary design phase. In this regard, four different levels of design and analysis maturity are identified that fall within the traditional conceptual, preliminary, and final design phases.

Figure 1, NASA CLV/CEV

2 Progressive analysis and design

Regardless if the design-to loads are quantified with or without FEA, an effective Progressive Design Process consists of three activities. All three activities can interact with each other throughout design maturation when they are automated and integrated.

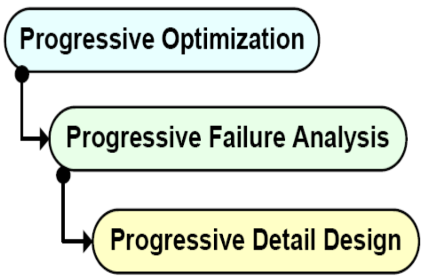

Fig. 3, A progressive process.

Progressive Optimization: A funneling process performed in stages to target an optimum design. Innovative "back to the drawing board" concepts are proposed, evaluated, and filtered out for the next stage of the design maturation process.

Progressive Failure Analysis: An incremental process of including more computationally demanding analysis solutions starting with damage initiation, tracking the progression of failure, and ending with the resulting residual strength at ultimate failure.

Progressive Detail Design: An incremental process of including more design detail, such as bonded and bolted joints, ply drop-offs, etc. for both optimization and analysis.

3 Global-local-detail process with the same FEM

A coarse meshed, loads model can accurately compute internal running design-to forces if the full definition of panel membrane, bending, and membrane-bending stiffness matrices are defined, including off diagonal terms, and entered into the element properties. This allows different panel concepts to be correctly modeled without the need for discretely meshing panel stiffener shapes, which would require

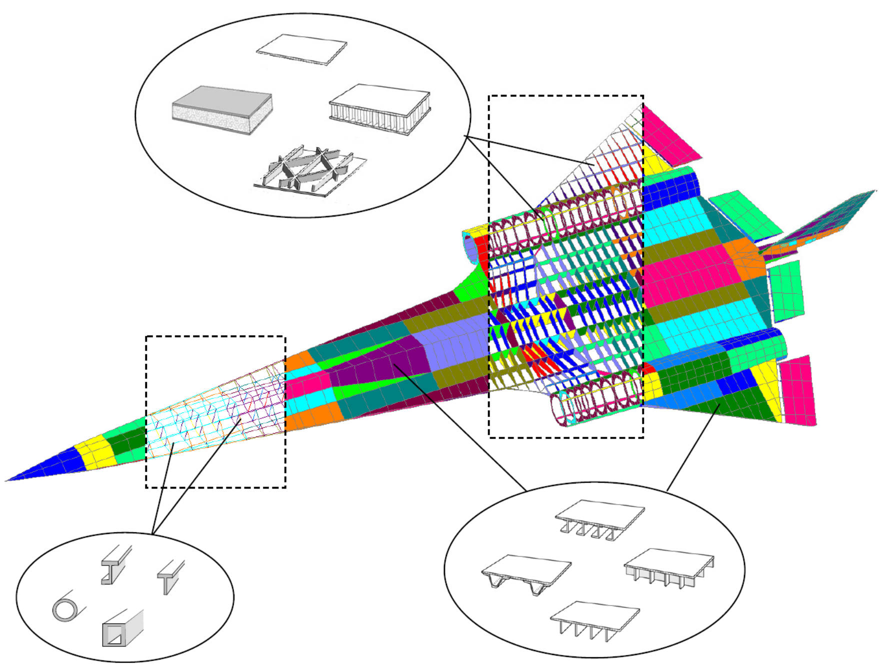

Fig. 4, A typical FEM of an early preliminary design modeled effectively and accurately with a coarse mesh of elements when higher fidelity thermoelastic stiffness terms are used to represent surface panels, and internal ribs and spars.

too many elements for surface acreage areas. Fig. 4, depicts the ability to quickly evaluate different panel concepts in this manner.

Once the loads are properly computed, then hundreds of different analyses such as panel buckling, crippling, beam-column, bonded and bolted joint, composite strength to damage initiation and damage tolerance criteria, etc. can be performed for the entire vehicle from engine nacelles to airframe surface panels and substructure. Fig. 3 illustrates how HyperSizer imports a FEM and manages all data associated with a configuration. Wing spars and ribs can consider a range of materials and panel concepts that are different than the subset of user determined design options for the wing skins and fuselage body. This process can include the analysis and sizing of internal beams such as spar caps and many other open and closed shapes. A primary foundational capability is to accurately analyze any panel concept without the need to discretely mesh with finite elements the shape of the stiffeners or their spacing. This permits tremendous flexibility and rapid turn around of trades with different panel concepts all from the same coarsely meshed FEM.

Fig. 5 represents a Global-Local-Detail process that very accurately determines ply-by-ply stresses throughout a panel's cross section. Starting with a vehicle FEM, an arbitrary location on the generated transparent graphic (a), is identified with surface skins as being Tee shaped stiffened panels (b), which are separated by an unstiffened web. Both are modeled in the global loads FEM with a single plane of elements. Note the mesh refinement does not have to align with the stiffener spacing and the user can construct the mesh with as few elements as appropriate to get overall running loads in the skins (b). The image depicts a 6 x 4 element mesh per panel bay, but for this specific model, only one element was needed to span the substructure, full depth webs. Each panel bay can be modeled with a single finite element because for any general, uniformly applied edge forces or moments including out-of-plane surface pressure, the approach can compute the resulting local panel deformation as portrayed at (c). This includes thermoelastic deformations caused by in-plane and out-of-plane temperature gradients. The process can automatically couple to FEA codes, and is FEA code independent. After the process has optimized the design of the vehicle, each user identified component will have its generalized temperature dependent stiffness terms updated in the FEM. This is accomplished by regenerating NASTRAN PSHELL and MAT2 data types for shell elements and PBAR and MAT1 for beams. With the new material and design data, another FEA is submitted for the next round on internal loads that capture changed load paths. At this point the software reads the new computed element forces from the FEA output file. In this manner, the optimizer can evaluate any stiffened panel cross sectional shape without having to remesh the model. Trades between honeycomb sandwich, blade stiffened, and/or hat stiffened panels are lightning fast.

There is no limit to the number of FEM elements, grids, or load cases, permitting the ability to rapidly handle large FEMs. A linear relationship between run times and model size is apparent, not exponential which can become detrimental when going from demonstration to full production FEMs.

Such an approach can analyze and optimize all structural components of entire airframes to thousands of load cases. Statistical post processing of the FEA computed element forces provide appropriate design-to loads. These loads are used for panel buckling and beam-column type failure analyses and are further resolved into individual panel segment forces, Fig 5 (d), for other instability analyses such as local buckling and crippling, and then even further for concentrated stresses/strains. Specializing in composite analyses and optimization, a progressive Global-Local-Detail process of computing stresses and strains allows hundreds of different failure analyses to be included. Material strength failure predictions for the laminates include the panel span segments (e, left image) and the bonded joint between skin and flange of a stiffened panel (e,right image).

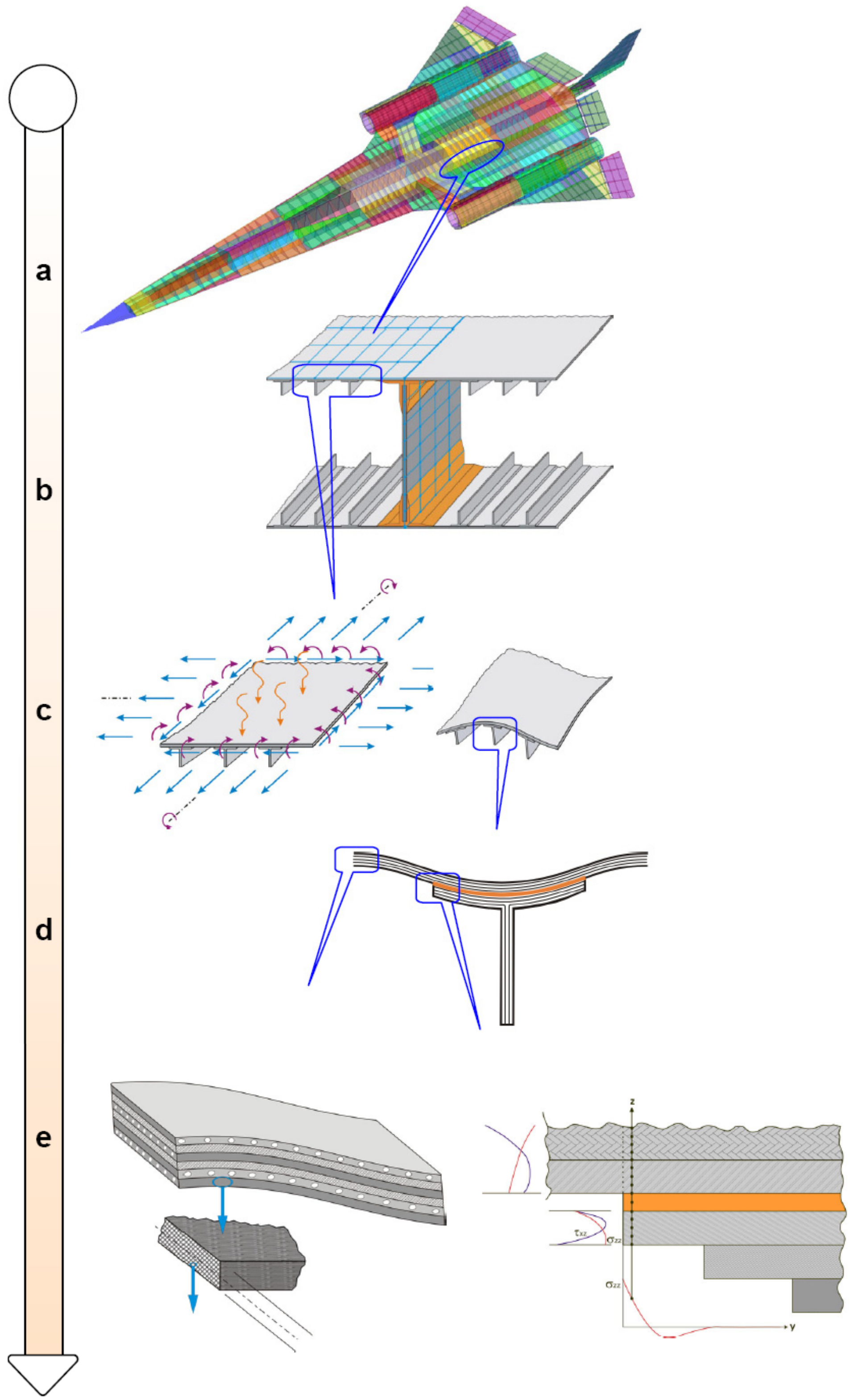

Fig. 5, A global-local-detail analysis process of drilling down to obtain interlaminar shear and peel stresses in each individual ply of a bonded joint.

Interlaminar shear and peel stress variation is computed in the adhesive for linear and five different non-linear material methods. The Z axis stress variation is also computed throughout the laminate depth, and also for each individual ply as required for the last ply of a stepped joint, (e, right). The number of integration points and characteristic distance for failure prediction can be selected by a user. In addition to material strength based on damage initiation, damage tolerance residual strength of strain energy release rates (SERR) are computed using a rapid, non-FEA, virtual crack closure technique (VCCT). These values are compared to critical energy release rates GIc and GIIc to predict delamination propagation for a crack between laminate plies and/or a crack between the skin and bonded flange.

Fig. 6 describes four progressive maturity levels for analysis and design optimization. Each of these correspond to a level of computational effort rather than a level of fidelity, although these often coincide.

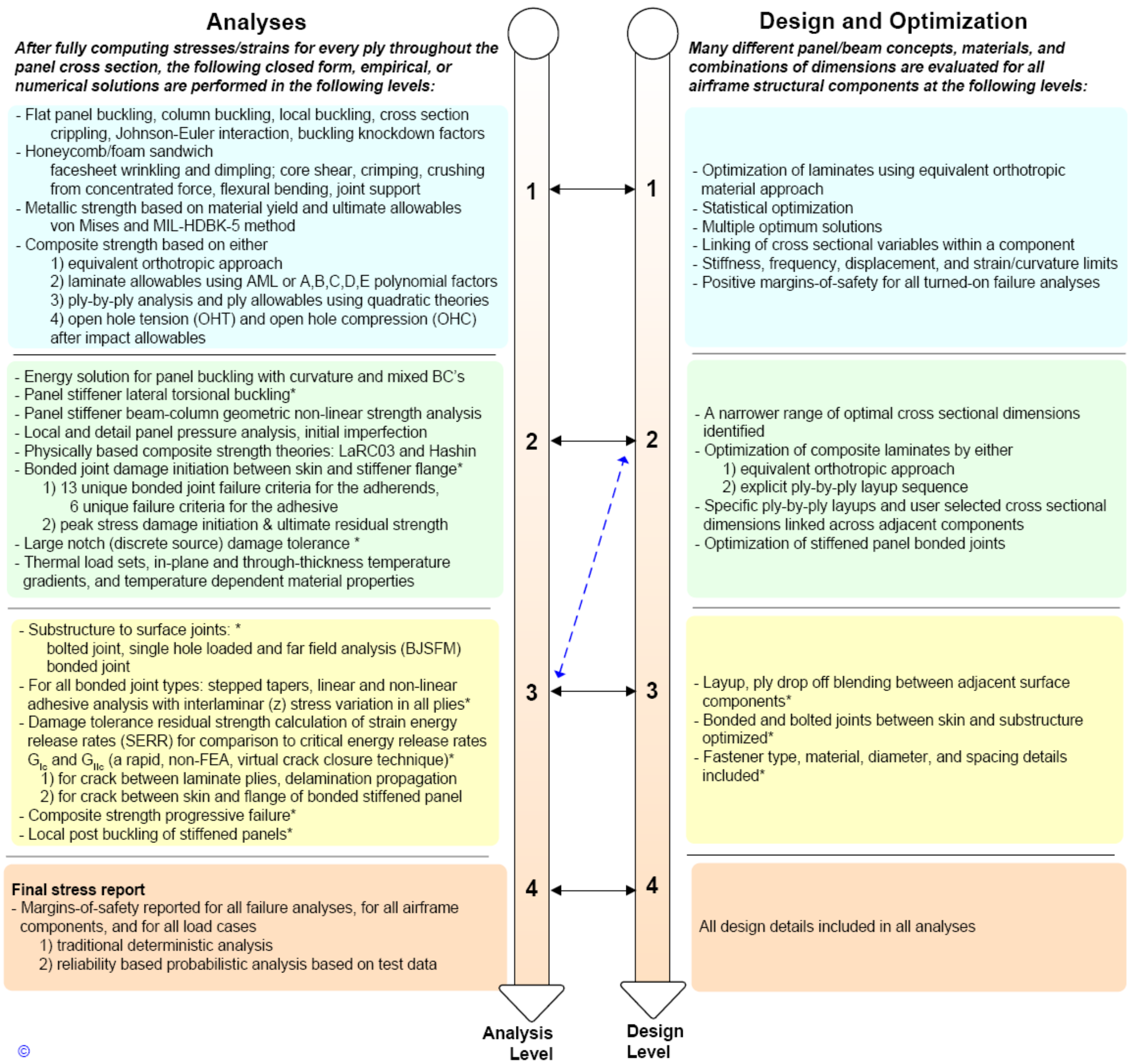

Fig. 6, Four levels of progressive design and analysis identified.

The intent is to pair the analysis and design levels to achieve the best efficiency of accuracy and optimization throughput. Overall accuracy is based on the analysis accuracy of each isolated failure prediction, as well as the breadth of failure modes included. An appropriate analysis process provides the flexibility to switch between levels (blue dashed line) for obtaining the most revealing and relevant time appropriate results.

Fig. 7 identifies how HyperSizer's four levels of extensive analyses and progressive optimization fit into the traditional phases of the aerospace engineering design process of conceptual, preliminary, and final design. The numbers represent a full fledged effort to extensively explore the design space. Throughout all levels, the quality of engineering knowledge and experience dramatically improves the results. The proportion of interactive user hours is higher in the earlier design phases where time is spent interpreting results and steering the optimization.

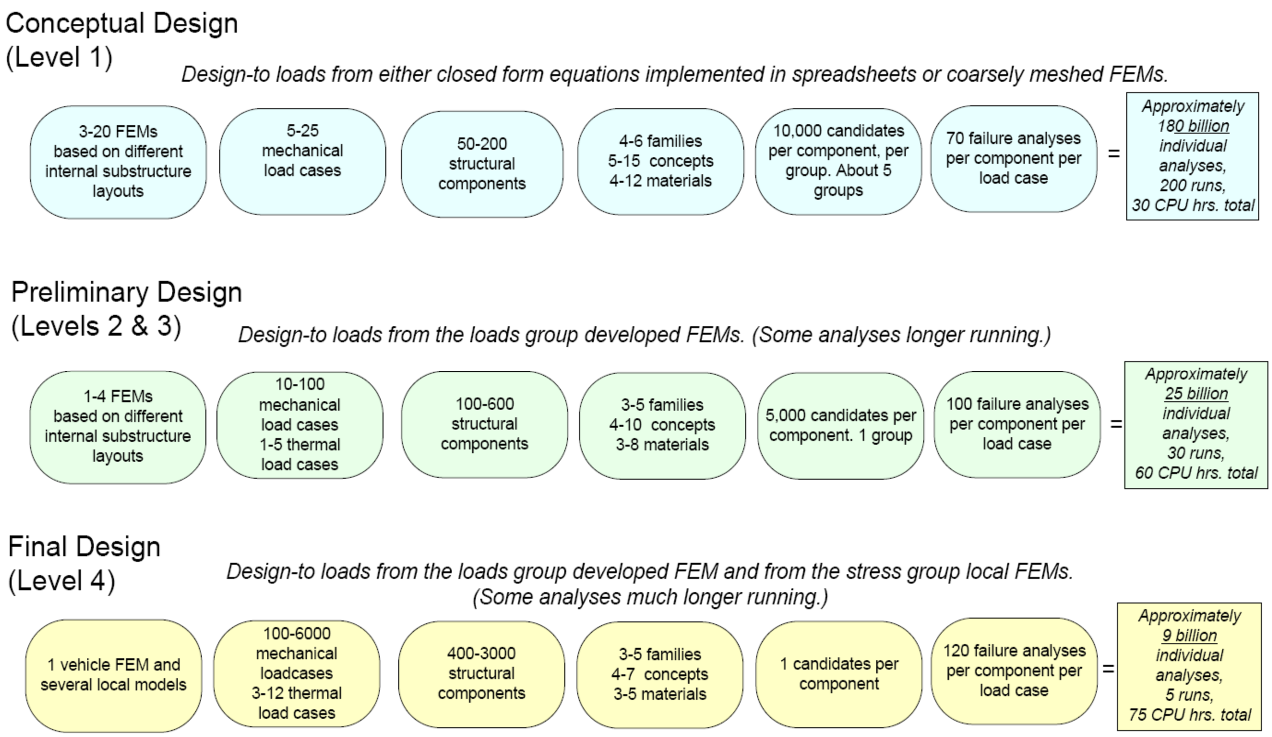

Fig. 7, The traditional three phases of design and associated design space exploration.

4 Global-local-detail process using different FEMs

The ability to quickly transition to more refined FEMs is also a necessary capability in a PD process. Shown in Fig 8 is a notional hypersonic vehicle with traditional substructure of fuselage ringframes and wing spars and ribs. The process starts with the global FEM of both the airframe and the propulsion system, left image. The colors represent fairly large acreage definitions of constant FEM properties. The middle image represents a FEM of just the propulsion system and the attaching wing. The right image represents a more refined model of the propulsion system with the inlet, combustor, and nozzle defined. In all these models, the same failure analysis methods, material properties, and FEA coupling process should be used to form a consistent path of data migration.

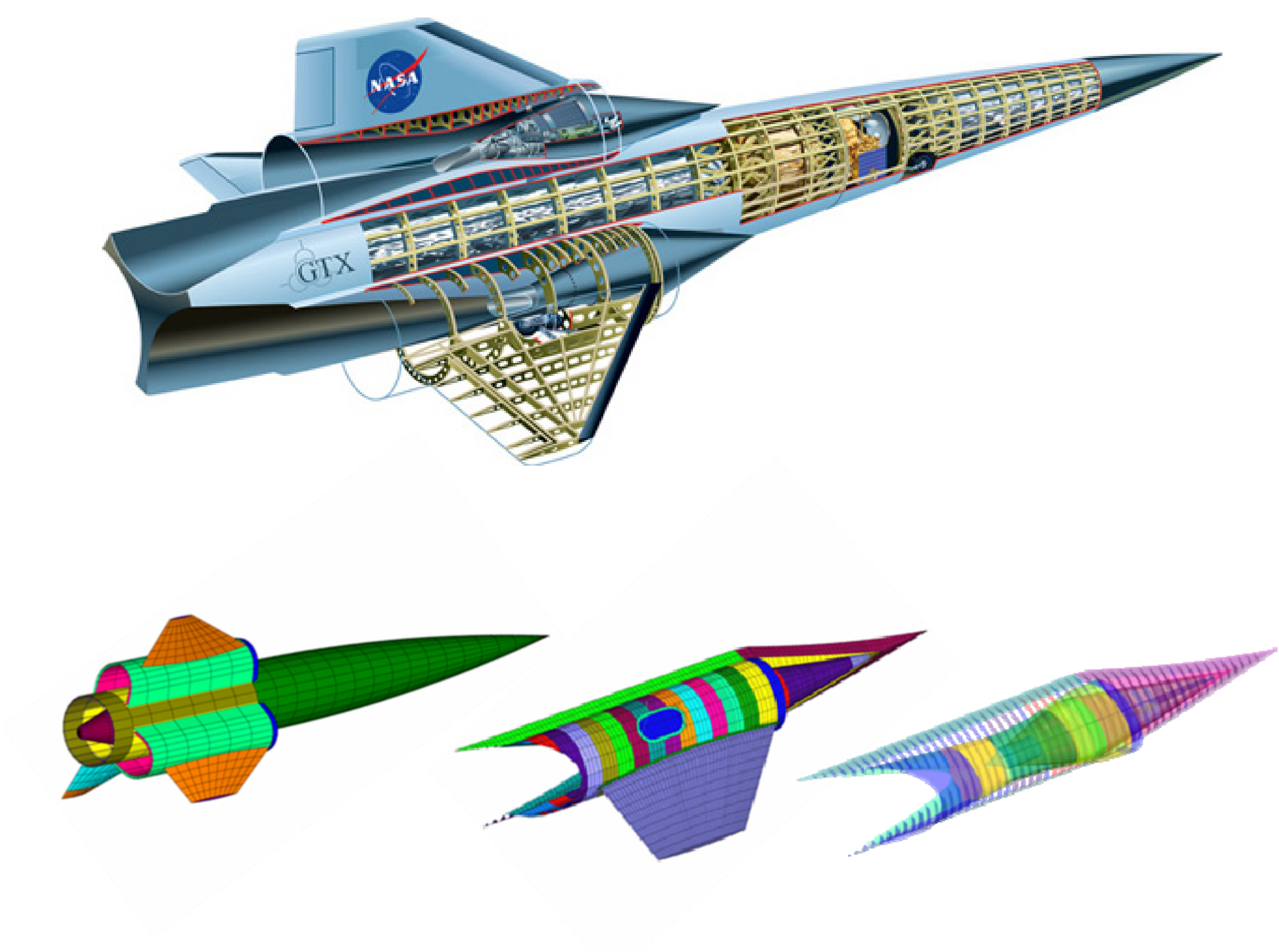

Fig. 8, Three different FEMs showing mesh refinement of structural components.

5 Wing box sizing optimization example

Using closed form equations for calculating panel bending moments and out-of-plane shears due to fuel pressure, an Excel spreadsheet can be used to control the optimization of the rib spacing. In this case the both panel and rib optimizations can be performed with the sizing tool per each rib spacing to generate weight curves for different loadings and boundary conditions. Fig. 9 graphs the results and aids in the visual determination of the proper rib spacing to use for the next step of FEM(s) creation. Unit weight, psf, on vertical axis and span distance horizontal axis, inches.

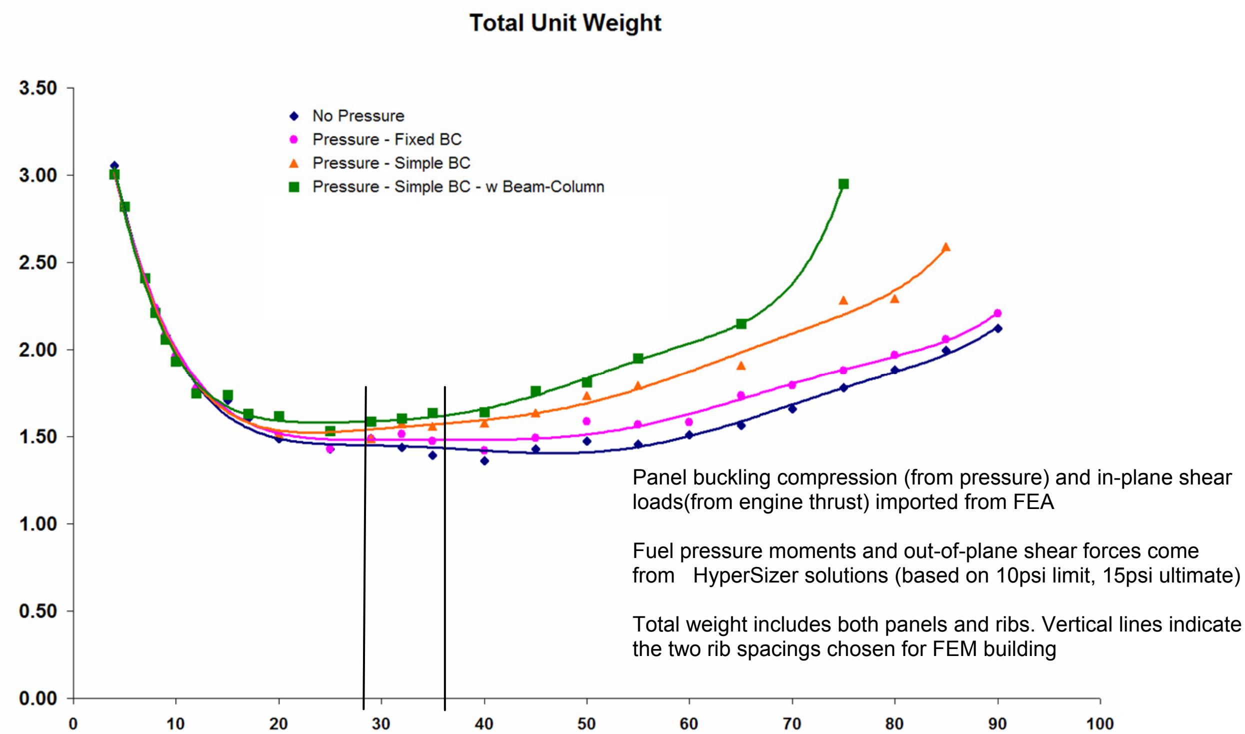

Fig. 9, When pressure effects and the resulting beam-column non-linear response is considered, the optimum rib spacing is seen to fall around 32" which closely matches traditional wing designs.

Once the wing rib spacing is established, then a FEM can be constructed and wing flight pressures, landing loads, etc. applied to it. Fig. 10 illustrates such a FEM. Fig 11 identifies the areas of constant element properties (structural components). In this case they are the panels that span the ribs. Elements that are of the same color are linked to the same FEM property data that defines its material, layup, thickness, etc. Six elements span between each rib. However, fairly accurate results could have also been obtained with a FEM that has five times fewer elements and grids than shown here. Therefore, instead of a 5000 element FEM, this could have been a 1000 element FEM.

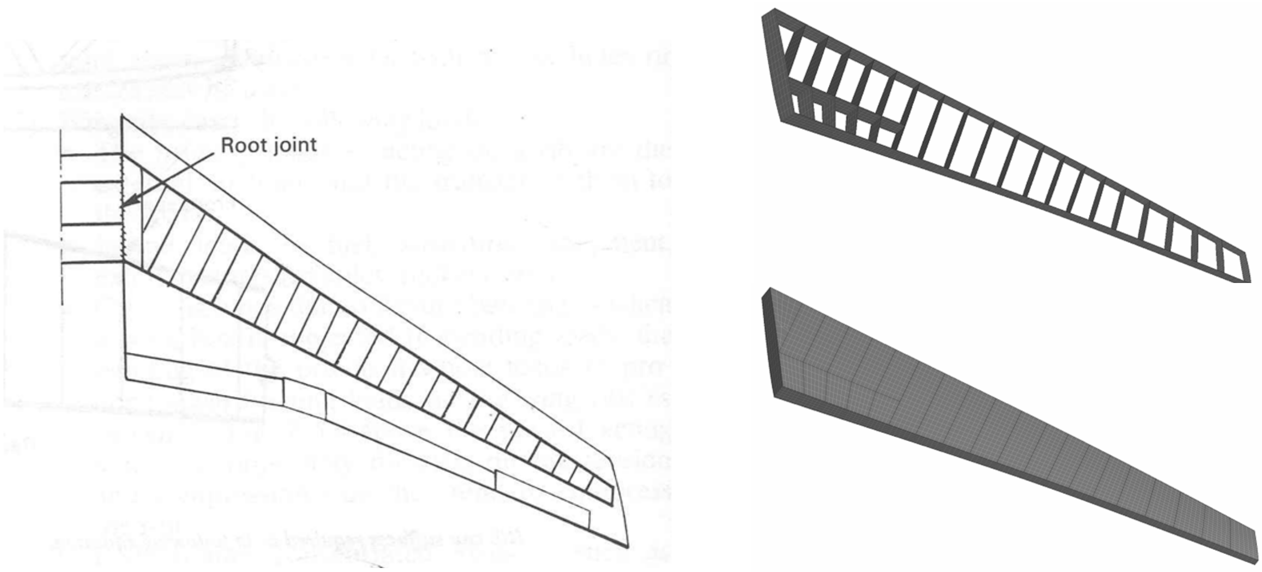

Fig. 10, The wing box spars and ribs as shown to the left image of a traditional transport wing, is modeled in the FEM with 29" rib spacing in the sweep direction. The top image shows the internal substructure, the bootm image the OML surface panels.

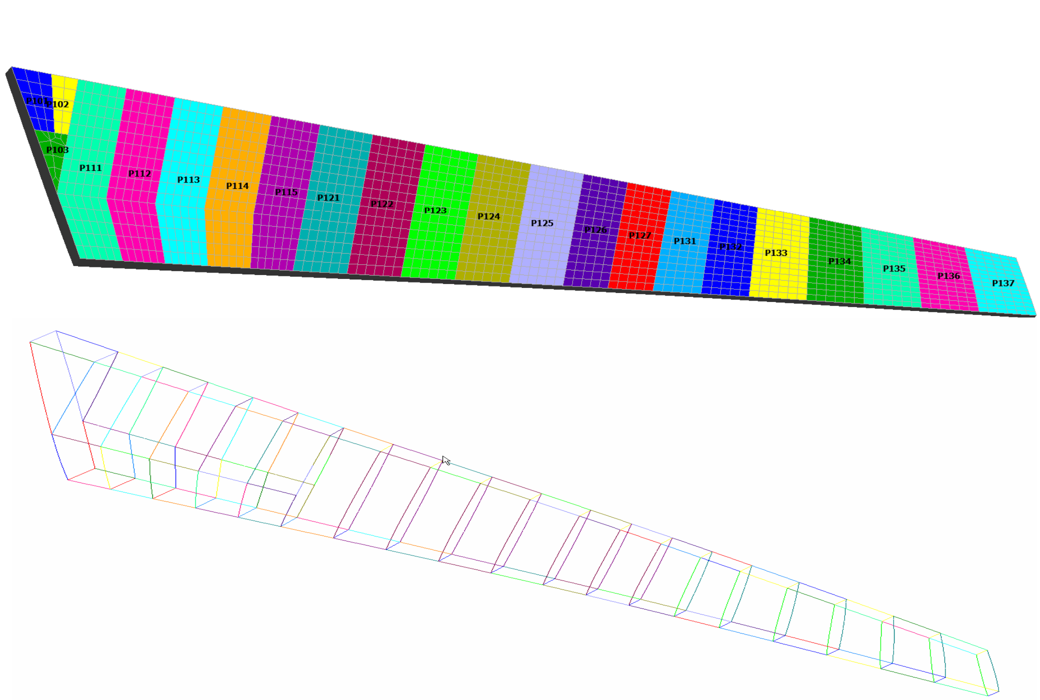

Fig. 11, The top image is the surface OML of shell elements and the bottom image is beam elements representing spar and rib caps. The colors represent areas of constant FEM property definition.

Once the external loads are applied and the FEA computes the running element forces, they are used to perform the strength and stability analysis of the OML surface panels and the internal substructure. Figures 12, 13, and 14 depict a small subset of the various results computed and plotted on the FEM.

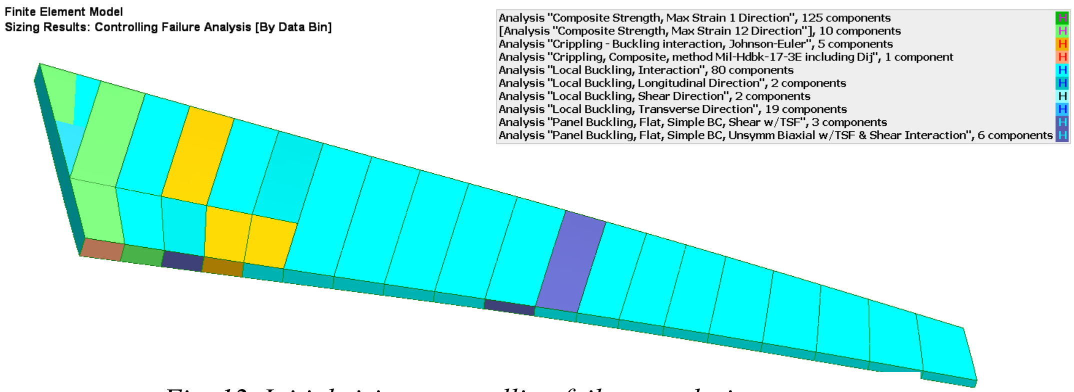

Fig. 12, Initial sizing, controlling failure analysis.

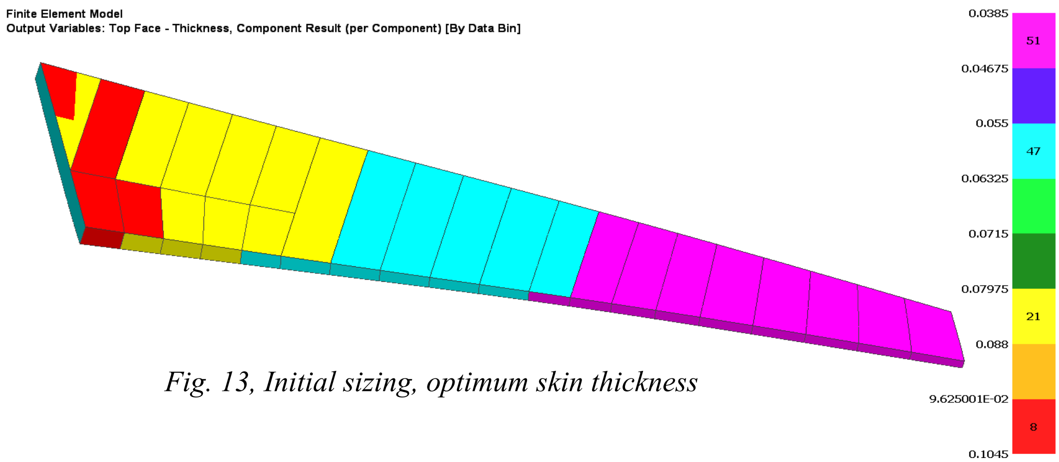

Fig. 13, Initial sizing, optimum skin thickness

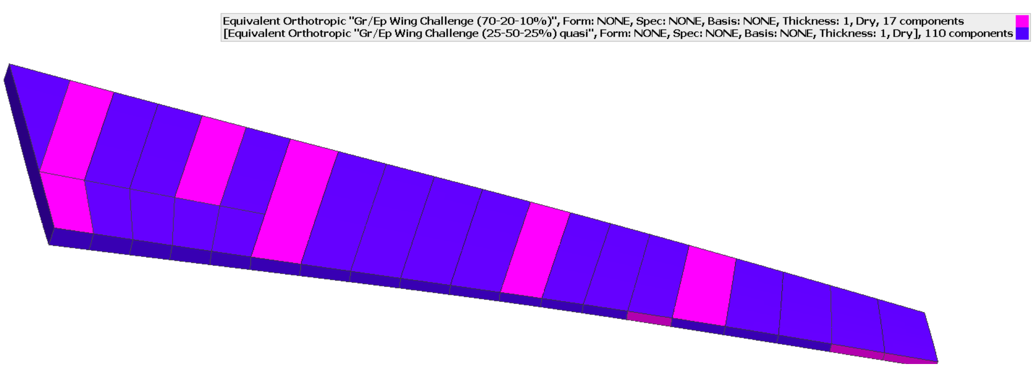

Fig. 14, Initial sizing, optimum layup percentage

The previous figures are based on first level analysis for the initial sizing. If the preliminary design were allowed to progress without including the more advanced analysis, then the design could be trapped into a difficult and costly situation of not obtaining positive strength margins during final design. For instance, Fig. 15, left image, shows all positive margins, but when the additional Beam-Column analysis is included, a large portion of the wing is shown to have negative margins, right image of Fig 15. However, if the sizing optimization includes beam-column during preliminary design where most of the variables are still open for change, then the weight impact of finding an alternate design that meets beam-column is only slightly heavier. In this case the weight went up only 1%.

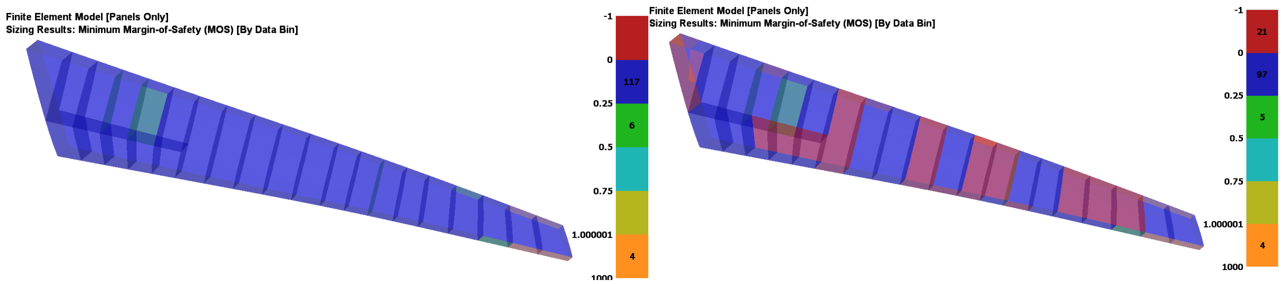

Fig. 15, Margins-of-safety: left all +MS working design, right several –MS (red color) after applying an additional failure analysis to the design

Fig 16 tells the same story, but this time with the effects of including bonded joint analysis of the panel stiffener. When the bonded joint analyses are included in the PD sizing process, then they too like beam-column, can be mitigated by finding an alternate design that satisfies them. In this case to achieve all positive margins caused a weight growth of 12%.

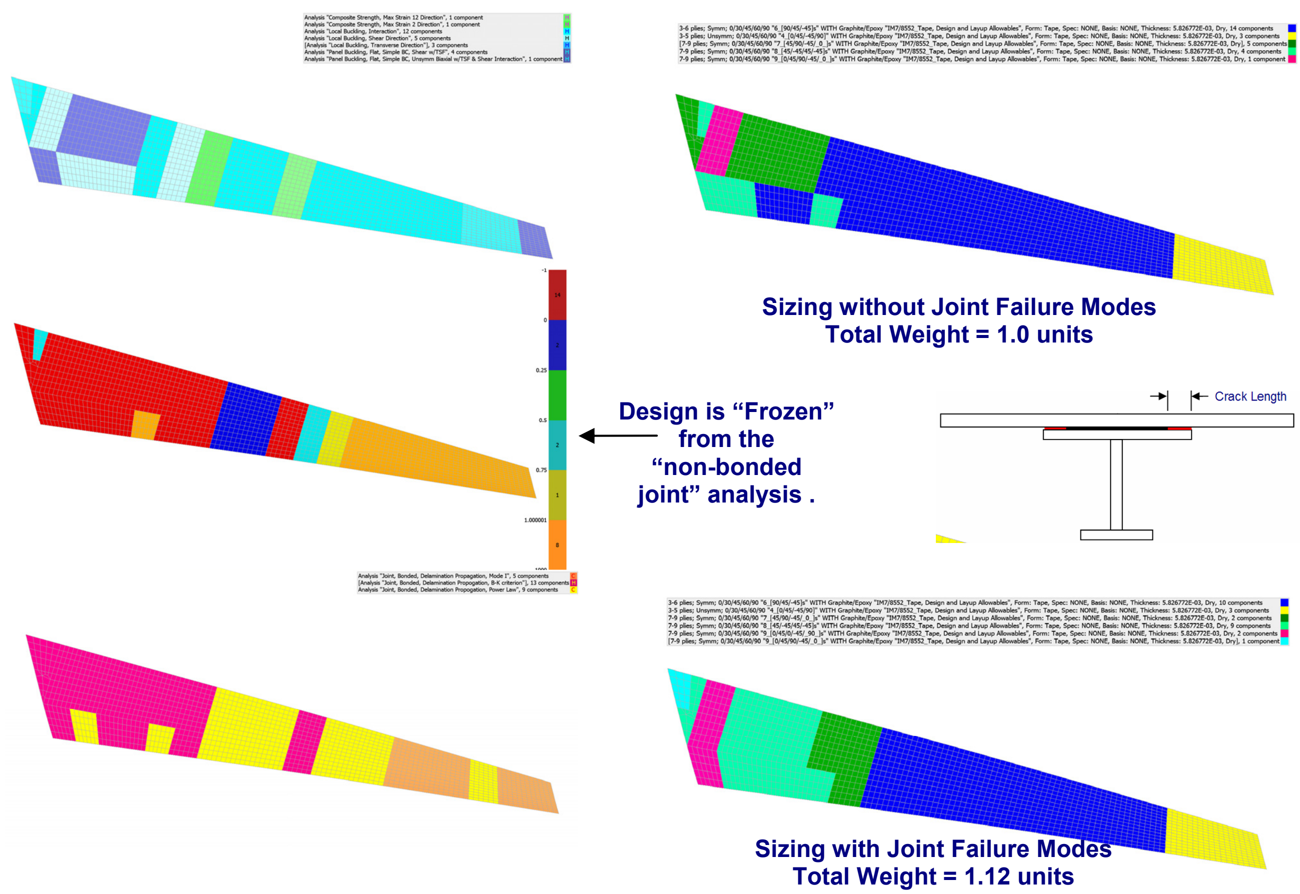

Fig. 16, The impact of not including bonded joint analysis in the preliminary design. The top left image shows controlling failure analysis before including bonded joint failure modes. When this design is frozen and the joint analyses are included, in this case damage initiation and damage tolerance crack growth analyses, then negative margins are apparent.

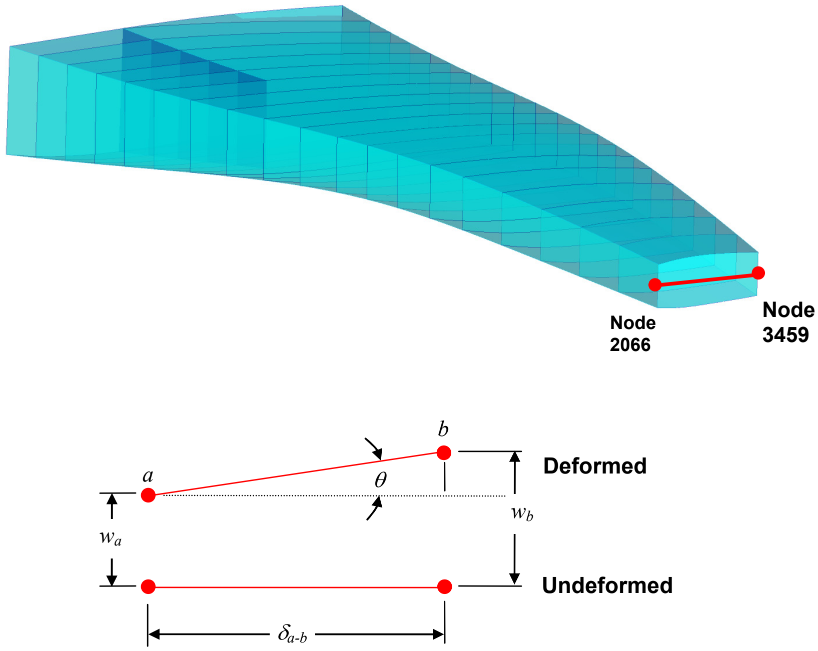

$$\theta = \tan^{-1}\left(\frac{w_b - w_a}{\delta_{a \to b}}\right)$$

Fig. 17, Function for calculating wing tip deflection and twist, theta.

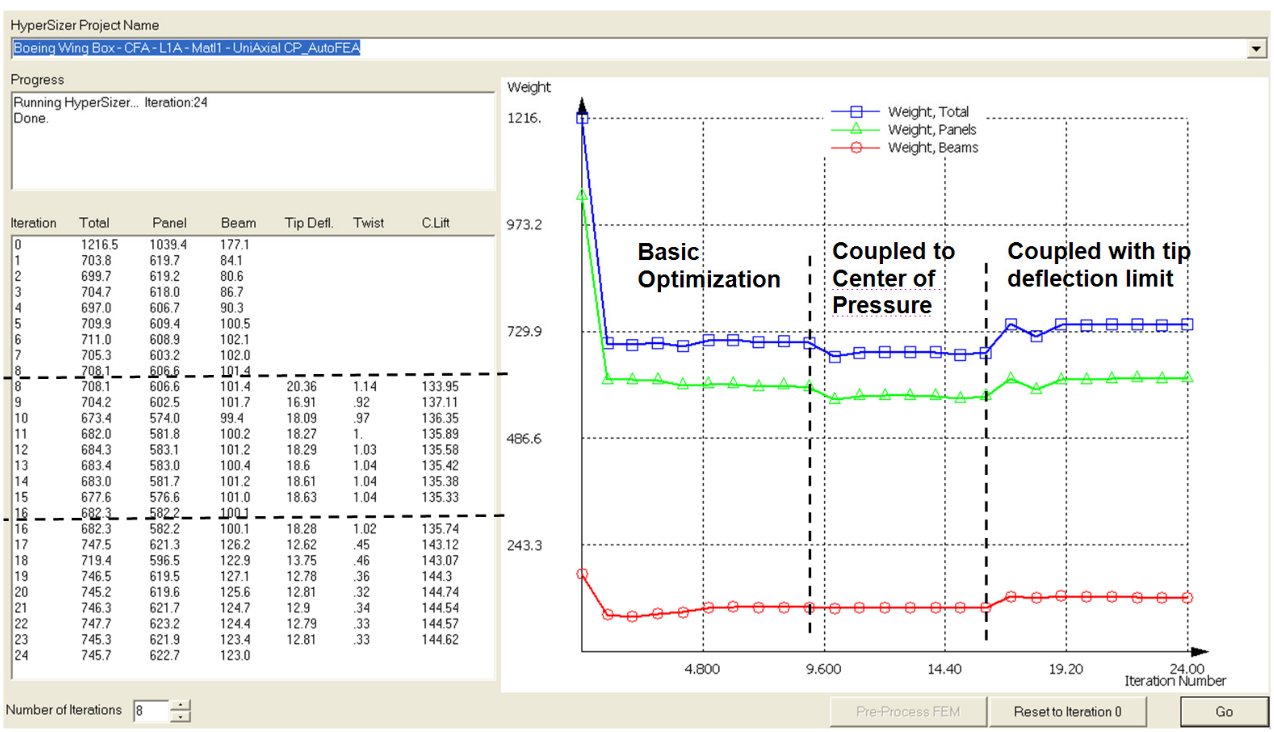

Iteration	Total	Panel	Beam	Tip Defl.	Twist	C.Lift
0	1216.5	1039.4	177.1			
1	703.8	619.7	84.1			
2	699.7	619.2	80.6			
3	704.7	618.0	86.7			
4	697.0	606.7	90.3			
5	709.9	609.4	100.5			
6	711.0	608.9	102.1			
7	705.3	603.2	102.0			
8	708.1	606.6	101.4			
8	708.1	606.6	101.4	20.36	1.14	133.95
9	704.2	602.5	101.7	16.91	.92	137.11
10	673.4	574.0	99.4	18.09	.97	136.35
11	682.0	581.8	100.2	18.27	1.	135.89
12	684.3	583.1	101.2	18.29	1.03	135.58
13	683.4	583.0	100.4	18.6	1.04	135.42
14	683.0	581.7	101.2	18.61	1.04	135.38
15	677.6	576.6	101.0	18.63	1.04	135.33
16	682.3	582.2	100.1			
16	682.3	582.2	100.1	18.28	1.02	135.74
17	747.5	621.3	126.2	12.62	.45	143.12
18	719.4	596.5	122.9	13.75	.46	143.07
19	746.5	619.5	127.1	12.78	.36	144.3
20	745.2	619.6	125.6	12.81	.32	144.74
21	746.3	621.7	124.7	12.9	.34	144.54
22	747.7	623.2	124.4	12.79	.33	144.57
23	745.3	621.9	123.4	12.81	.33	144.62
24	745.7	622.7	123.0			

Fig. 18, Red indicates beam weight, green panel weight, and blue total weight as a function of iteration number between FEA and the sizing process.

Fig. 17 illustrates the wing box in a perspective that permits the wing box tip to be seen. Two nodes are identified as control points for the purpose of calculating wing deflection and twist and for the purpose of limiting this aeroelastic deformation. The wing twist is defined with the function and represented as theta. Fig. 18 is a graph of converged weight as a function of iteration number between the sizing process and FEA. Note as the process is started, the design is heavy and within one iteration with the sizing software is reduced and essentially converged on total weight. At iteration number 8, the twist function is used to update the center of lift pressure, in this case causing it to move closer to the fuselage and relieving the design-to, cantilevered induced membrane forces. This reduced force allows the sizing process to be lighter (iterations 8 through 16). At iteration 16, an arbitrary limit on tip deflection of 12" was imposed. This caused the design to be heavier to meet this additional stiffness. The weight went up about 9%.

6 Conclusions

An automated process for analysis and sizing is very valuable in the preliminary design phase of a project. As many high fidelity analysis as possible should be included in preliminary design to produce hardware concepts that have the best chance for less weight growth during final design. By including these analyses early on, their weight impact can be lessened by finding appropriate alternate designs. The HyperSizer and HyperFEA software has been presented for this purpose.

7 Acknowledgments

This material is based upon work partially supported by the United States Air Force under Contract.

1. AFRL VA SBIR Phase I contract # F33615-01-M-3125
2. AFRL VA SBIR Phase II contract # F33615-02-C-3216
3. NASA SBIR Phase I contact

8 References

1. Phase I Final Report for Air Force Research Lab (AFRL) SBIR AF01-239, Certification of Aerospace Structures by Analysis, Collier Research Corporation December 2001

2. Collier, Craig, Veley, Duane, and Owens, Steve, "Virtual Testing with Validated Analysis Tools," NATO AVT symposium in Paris, France, April 2002

3. Collier Research Corporation, SBIR Final Report: Consistent Structural Integrity and Efficient Certification with Analysis, Air Force Research Lab (AFRL) SBIR Phase II contract # F33615-02-C-3216 Volumes 1, 2, and 3, October 2004